AIAA 81-4253

Self-Induced Separation of Flow in a Hydrodynamic Scoop

Gustave Hokenson*
Dynamics Technology, Inc., Torrance, Calif.

Abstract

FLOW through a hydrodynamic scoop which imparts an angular deflection to the oncoming fluid stream is studied both theoretically and experimentally. The analytical model proposes strongly interacting, yet distinct, inviscid and boundary-layer flow structures. Analysis is carried out for two-dimensional flows for which approximate closed-form results can be obtained. Theoretical prediction of the optimal scoop configuration and efficiency is obtained as a function of the deflection angle, entrance Reynolds number, and length scale. In addition, the flow coherence is found to degenerate into a spray at the point of optimal efficiency, when self-induced flow separation is established within the scoop. Utilizing a length scale correlation, the two-dimensional model is extended to predict the experimental performance and spray transition boundary of optimal three-dimensional scoops. Experimental confirmation of the analytical model motivates the consideration of porous wall scoops, that inhibit the transition to spray.

Contents

Flowfield Description

The two-dimensional scoop selected for investigation is depicted in Fig. 1, which illustrates the flowfield free surface (R_1) and boundary-layer edge (δ; $R_2 \equiv R_c - \delta$) relative to the scoop wall (R_c). Experimental observations† indicate that, for a given scoop geometry as defined by its curvature R_c^{-1}, the flow pattern and performance is sensitive to the thickness Δ of the fluid layer that is "skimmed off" the free surface. The fluid stream is picked up, turned/distorted, and ejected by the scoop in an orderly manner for a restricted range of $\bar{\Delta}(\equiv \Delta/R_c)$ values. Beyond this range, the fluid stream coherence is lost and a spray field ensues, with consequent reduction in the magnitude of reaction forces.

Simplified Analytical Model

According to the analytical model,[1-8] a rectilinear flow is skimmed off the free surface and transitions over a specified length L_0 to a curvilinear structure with the concurrent generation of a radial pressure gradient, flowfield distortion, and free-surface displacement toward the center of curvature. As the boundary layer grows on the inner surface of the scoop, it further displaces the free surface and increases the self-induced pressure. This is computed with a coupled integral boundary layer-inviscid flow analysis assuming similar velocity profiles. Providing $\bar{\Delta}$ is large enough, or the scoop wetted length L is long enough relative to the entrance boundary-layer momentum thickness θ_0, the flow will separate from the inner surface. Separation at the exit plane is specified to represent the spray transition boundary.

The proposed analytical model explains the experimentally-measured high scoop efficiency. From the entrance plane to the maximum pressure point, frictional stresses decrease as the average pressure builds and the film thickens to accommodate a reduced mean velocity. Therefore, the scoop serves as an efficient device to store the entering kinetic energy. Provided separation does not occur before the flow "senses" the streamline straightening and negative pressure gradient near the exit plane, the positive pressure then accelerates the thick layer of relatively low velocity fluid through a *short* effuser. This efficiently reconverts the stored pressure energy to kinetic energy in a new vector direction, with the resultant force applied to the scoop.

For any scoop to operate optimally (i.e., near the spray transition boundary), yet stably, the utility of a porous scoop wall is indicated by the analytical model. In such a device, self-modulated surface mass transfer inhibits the wall shear from becoming zero or negative. The mass transfer is passively controlled by the wall porosity and local fluid pressure, which increases and is a maximum at the point of incipient separation, precisely where removal of low momentum fluid is required.

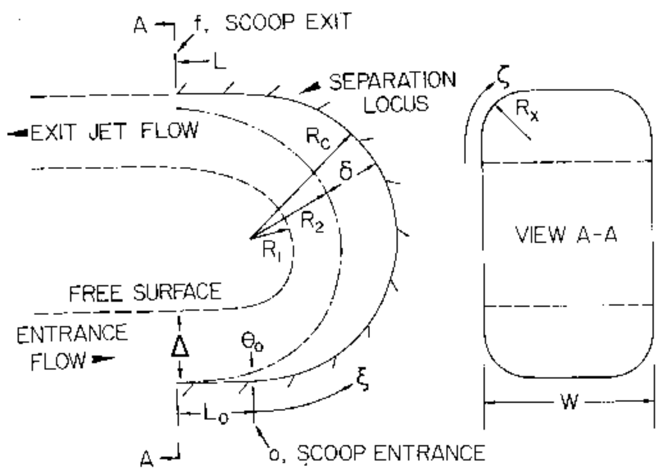

Fig. 1 Schematic representation of two-dimensional scoop planform geometry/flowfield and corresponding three-dimensional scoop frontal configuration.

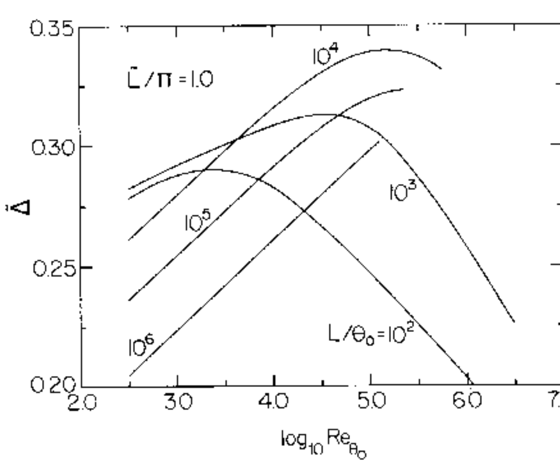

Fig. 2 Optimal scoop inlet film thickness as a function of Reynolds number for a 180-deg scoop turn ($\bar{L}/\pi = 1.0$) and various scoop lengths L/θ_0.

Synoptic submitted July 18, 1980; revision received March 18, 1981. Full paper available from National Technical Information Service, Springfiled, Va. 22151 at the standard price (available upon request).

*Senior Research Scientist. Member AIAA.

†All references to experimental or analytical results are documented in the full paper.

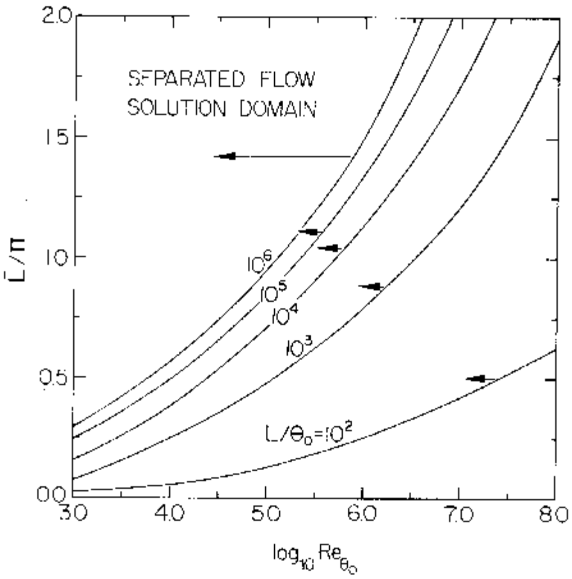

Fig. 3 Optimal scoop turn angle boundary of the separated flow solution domain as a function of Reynolds number for various scoop lengths L/θ_0.

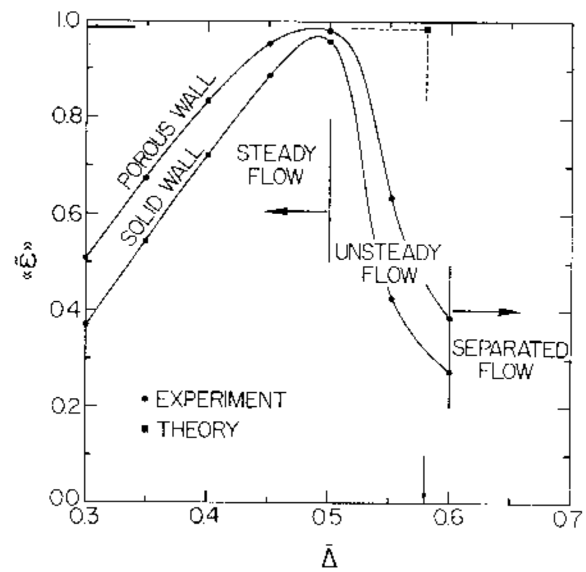

Fig. 4 Scoop energetic efficiency as a function of inlet film thickness for a 180-deg deflection angle ($\tilde{L}/\pi = 1.0$) with $L/\theta_0 = 10^3$ and $Re_{\theta_0} = 5\times10^2$.

Analytical Results

The flowfield solution has been obtained for a range of Reynolds numbers, scoop lengths, and deflection angles. For a 180 deg deflection ($\tilde{L}/\pi = 1.0$), the $\tilde{\Delta}$ results are presented in Fig. 2 as a function of Reynolds number for various values of L/θ_0. Note that, for each L/θ_0, $\tilde{\Delta}$ attains a maximum value in the middle of the Reynolds number range. In addition, for a given Re_{θ_0}, $\tilde{\Delta}$ is a maximum at an intermediate L/θ_0, with the overall maximum of 0.34 occurring at approximately $Re_{\theta_0} = 10^5$ and $L/\theta_0 = 10^4$.

Not all of the solutions that were sought admitted separation within the required flowfield constraints. The boundaries of the separated flow solutions are indicated in Fig. 3. The nonseparating high Reynolds number flow region increases with L/θ_0. However, for any value of $\tilde{L}$, sufficiently large $\tilde{\Delta}$ values cause a rupture of the fluid stream even for an Re_{θ_0} that lies to the right of the appropriate L/θ_0 boundary. This is due to normal impingement on the scoop deflection surface and is outside the context of the flowfield model developed here. For most cases of interest, a separated flow solution exists.

Experimental Results

Based on analysis, an optimal three-dimensional scoop ($\tilde{L}/\pi = 1.0$) was tested at $Re_{\theta_0} = 5\times10^2$ and $L/\theta_0 = 10^3$. The results, presented in Fig. 4, illustrate the dependence of scoop energetic efficiency $\langle\langle\hat{\epsilon}\rangle\rangle$ on the relative thickness of the entering film, for both a solid and porous wall scoop. The analytical results predict both the experimentally measured optimum scoop efficiency and the separation boundary with reasonable accuracy. However, the steady flow theoretical model cannot represent the transient flow phenomena observed between incipient and full separation. The experimental results were correlated to theory by identifying the two-dimensional $\tilde{\Delta}$ with the three-dimensional wetted surface length to flow area at the inlet plane.

Note that degradation in scoop performance caused by the onset of spray transition is delayed by the porous wall mass transfer. The efficiency of the porous scoop is enhanced at off-design conditions by improving the flow uniformity and increases, as per analysis, at the maximum efficiency point due to the increased $\tilde{\Delta}$.

Conclusions

Experimental verification of the analytical results substantiates the viscous/inviscid interacting flow model. Its validity is limited only by the values that Re_{θ_0} and L/θ_0 can assume yet still support incipient boundary-layer separation within the scoop, as required by the optimality constraint. Inasmuch as the analysis was generated on the assumption that the spray transition boundary may be defined by boundary-layer separation at the exit plane, this hypothesis has been verified. Finally, methodologies to arrive at unique solutions (for both solid and porous wall scoops) and apply them to general multidimensional configurations have been established.

References

[1] Lowy, R., "Efficiency Analysis of Pelton Wheels," *Transactions of the ASME*, Aug. 1944, pp. 527-538.

[2] Bradshaw, P., "Effects of Streamline Curvature on Turbulent Flow," AGARDograph No. 169, Aug. 1973.

[3] Hokenson, G., "Inverse Design of Optimal Diffusers with Experimental Corroboration," *Journal of Fluids Engineering*, Dec. 1979, pp. 478-482.

[4] Smith, F.T., "Upstream Interaction in Channel Flows," *Journal of Fluid Mechanics*, Vol. 79, Pt. 4, March 1977, pp. 631-656.

[5] Castro, I.P. and Bradshaw, P., "The Turbulence Structure of a Highly Curved Mixing Layer," *Journal of Fluid Mechanics*, Vol. 73, Pt. 2, Jan. 1976, pp. 265-304.

[6] So, and Ronald, M.C., "A Turbulence Velocity Scale for Curved Shear Flows," *Journal of Fluid Mechanics*, Vol. 70, Pt. 1, July 1975, pp. 37-57.

[7] Stewartson, K. and Williams, P.G., "Self-Induced Separation," *Proceedings of the Royal Society*, A, Vol. 312, 1969, p. 181.

[8] Stewartson, K. and Williams, P.G., "Self-Induced Separation," *Mathematika*, Vol. 20, 1973, p. 98.